



Rubino, S. and Bojoi, R. and Odhano, S.A. and Zanchetta, Pericle (2017) Model predictive Direct Flux Vector Control of multi three-phase induction motor drives. In: 2017 IEEE Energy Conversion Congress and Exposition (ECCE), 1-5 October 2017, Cincinnati, Ohio, USA.

Access from the University of Nottingham repository:

<http://eprints.nottingham.ac.uk/50466/1/Model%20predictive%20Direct%20Flux%20Vector%20Control%20of%20multi%20three-phase%20induction%20motor%20drives.pdf>

Copyright and reuse:

The Nottingham ePrints service makes this work by researchers of the University of Nottingham available open access under the following conditions.

This article is made available under the University of Nottingham End User licence and may be reused according to the conditions of the licence. For more details see: http://eprints.nottingham.ac.uk/end_user_agreement.pdf

A note on versions:

The version presented here may differ from the published version or from the version of record. If you wish to cite this item you are advised to consult the publisher's version. Please see the repository url above for details on accessing the published version and note that access may require a subscription.

For more information, please contact eprints@nottingham.ac.uk

Model Predictive Direct Flux Vector Control of Multi Three-Phase Induction Motor Drives

S. Rubino, R. Bojoi
Department of Energy
Politecnico di Torino
Torino, 10129, Italia

S. A. Odhano, P. Zanchetta
Department of Electrical and Electronic Engineering
University of Nottingham
Nottingham, NG7 2RD, United Kingdom

Abstract—A model predictive control scheme for multiphase induction machines, configured as multi three-phase structures, is proposed in this paper. The predictive algorithm uses a Direct Flux Vector Control scheme based on a multi three-phase approach, where each three-phase winding set is independently controlled. In this way, the fault tolerant behavior of the drive system is improved. The proposed solution has been tested with a multi-modular power converter feeding a six-phase asymmetrical induction machine (10kW, 6000 rpm). Complete details about the predictive control scheme and adopted flux observer are included. The experimental validation in both generation and motoring mode is reported, including post open-winding fault operations. The experimental results demonstrate the feasibility of the proposed drive solution.

Keywords—multiphase induction machines; multiphase drives; model predictive control; fault-tolerance; direct flux vector control

I. INTRODUCTION

In the recent years, the model predictive control (MPC) of the electrical drives has gained an impressive attention. In this context, a relevant development has been reached in the predictive torque control [1-6] that presents several advantages. Its most salient feature is the improvement of the dynamic torque response, generally better than traditional feedback controls [3]. Another aspect is a less demanding calibration of the control parameters and settings [6]. On the other hand, the use of predictive algorithms requires a good estimation of the machine's parameters and, in general, a greater computational power with respect to traditional control strategies. In this field of the research, an advanced development has been reached in the Finite Control Set Model Predictive Control (FCS-MPC) for three-phase machines [2-6]. With FCS-MPC, the voltage references are chosen from the instantaneous discrete states of the power converter to minimize a user-defined cost function.

Important limitations on the use of FCS-MPC schemes consist in the current's derivatives that can reach uncontrollable values, especially with low impedance machines (for example in traction motors). In fact, the behavior of the FCS-MPC is very similar to the well-known Direct Torque Control (DTC) implemented at low switching frequencies.

Another problem is the application of the finite-set methods on multiphase machines because they require a very high computational power of the dedicated control hardware. In the multiphase systems, the number of power converter's discrete states becomes very high [7-9], therefore the minimization of a cost function for every sample time (in many cases is the same or a half of the switching period) is less viable.

A possible solution to solve these issues can be the adoption of a continuous control set model predictive control (CCS-MPC). The main difference with respect to the classical finite-set types is the selection of the voltage references. In fact, it is performed in the range of all possible average voltage vectors, which the power converter can apply. This control strategy is usually known as modulated model predictive control (M²PC) using Pulse-Width or Space Vector Modulation [6] (PWM or SVM). Another predictive solution based on average voltage vectors applied at constant switching frequency is the Dead-Beat Direct Torque and Flux Control (DBTFC). As example, the solution presented in [10] for three-phase induction machines contains a deadbeat control law based on a Volt-second-based torque model to produce the desired torque and stator flux magnitude simultaneously.

The literature reports a few predictive control solutions applied to multiphase induction drives. The solution presented in [9] is related only to the current control using FCS-MPC of an asymmetrical six-phase induction machine prototype exhibiting high inductance values.

The goal of the work is to propose a model predictive control for multiphase Induction Motor (IM) drives configured as multi three-phase units. The proposed strategy uses the voltage and current range of the power converter with no issues related to uncontrollable current's derivatives for low impedance machines. The predictive algorithm is implemented on the basic structure of the Direct Flux Vector Control (DFVC) scheme for simultaneous flux and torque control. The performance of the proposed control has been validated with a 10 kW@6000 rpm asymmetrical six-phase induction machine using a double-three-phase stator winding configuration.

The paper is organized as follows. The description of the drive topology and machine modeling are analyzed in Section II. The formulation of the model predictive algorithm is described in Section III. The proposed predictive control scheme is described in Section IV, while the test rig and the experimental results are provided in Section V.

II. MULTIPHASE TOPOLOGY AND MACHINE MODELING

A. Multi Three-Phase Topology

The multi three-phase topology uses multiple independent three-phase units (Fig. 1). The stator consists of independent three-phase windings with isolated neutral points.

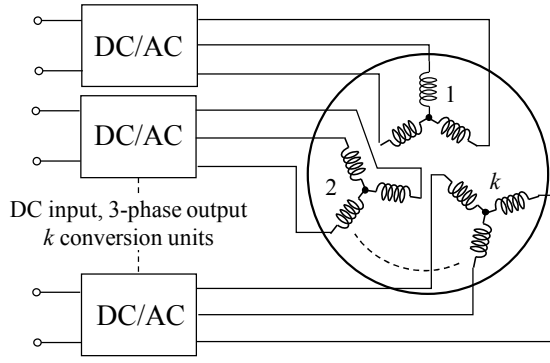


Fig. 1. Multiphase topology with multiple three-phase units.

In this configuration, each three-phase set is supplied by an independent three-phase inverter. The inverter units share the control algorithm only at high level to obtain full fault-tolerance.

If a three-phase inverter unit goes in fault, it is disconnected from the DC power supply. The main advantage of this configuration is the use of the well-consolidated three-phase power electronics modules, reducing the converter size, cost and design time [11].

B. Machine Modeling

The mathematical description of the multi three-phase topology can be performed by using the Multi-Stator (MS) approach. Introduced in [12] and recently applied in [13] for a quadruple-three phase machine, it considers the stator as a multiple of three-phase set, while the rotor is seen as a three-phase structure [14].

This section presents a generic MS modeling approach for an Induction Machine (IM) with the hypothesis of sinusoidal distribution. The number of phases of the machine is $nph=3n$ and $k=1,2,\dots,n$ is the index number of a single three-phase set. The stator parameters of the three-phase sets are considered different each other in order to deal with the most general case. For simplicity, the iron losses are neglected.

For each three-phase stator k -set, the stator voltage equations are:

$$[v_{sabc,k}] = R_{sk} \cdot [i_{sabc,k}] + \frac{d}{dt} [\lambda_{sabc,k}] \quad (1)$$

where: $[x_{sabc,k}] = [x_{sak} \ x_{sbk} \ x_{sck}]^t$ is a stator vector defined for the three-phase set $(abc)_k$ and defined in own stator coordinates;

R_{sk} is the stator resistance for the three-phase set k .

Assuming a rotor cage that is equivalent to a three-phase wound rotor, the rotor voltage equations are:

$$[v_{rabc}] = [0] = R_r \cdot [i_{rabc}] + \frac{d}{dt} [\lambda_{rabc}] \quad (2)$$

where: $[x_{rabc}] = [x_{ra} \ x_{rb} \ x_{rc}]^t$ is a rotor vector in rotor phase coordinates;

R_r is the rotor resistance.

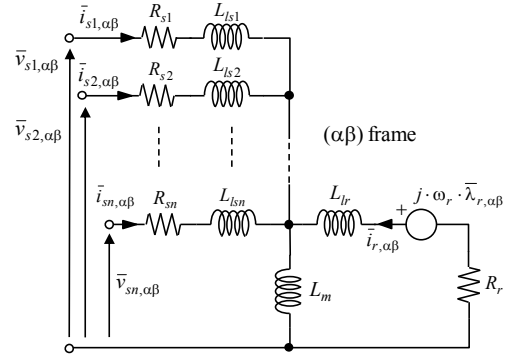


Fig. 2. Equivalent circuit of IM in stationary (α,β) frame.

The IM magnetic model is described by (3) and (4):

$$[\lambda_{sabc,k}] = L_{lsk} \cdot [i_{sabc,k}] + \sum_{z=1}^n ([M_{sk-sz}] \cdot [i_{sabc,z}] + [M_{sk-r}] \cdot [i_{rabc}]) \quad (3)$$

$$[\lambda_{rabc}] = L_{lr} \cdot [i_{rabc}] + \sum_{z=1}^n ([M_{r-sz}] \cdot [i_{sabc,z}] + [M_{r-r}] \cdot [i_{rabc}]) \quad (4)$$

where: $[M_{sk-sz}]$ is a 3×3 mutual inductance matrix between two stator windings;

$[M_{sk-r}]$ is a 3×3 mutual inductance matrix between the stator windings of k set and the rotor;

$[M_{r-sz}]$ is a 3×3 mutual inductance matrix between the rotor and the stator windings of z set;

$[M_{r-r}]$ is a 3×3 mutual rotor inductance matrix;

L_{lsk} is the stator leakage inductance for the three-phase set k ;

L_{lr} is the rotor leakage inductance.

All rotor parameters from (2-4) are referred to the stator.

The MS approach needs the application of the general Clarke transformation to get the machine model in stationary (α,β) frame:

$$[T_k] = \frac{2}{3} \cdot \begin{bmatrix} \cos(\vartheta_k) & \cos(\vartheta_k + 2\pi/3) & \cos(\vartheta_k - 2\pi/3) \\ \sin(\vartheta_k) & \sin(\vartheta_k + 2\pi/3) & \sin(\vartheta_k - 2\pi/3) \\ 1/2 & 1/2 & 1/2 \end{bmatrix} \quad (5)$$

where ϑ_k is the angle considered for a three-phase k -set; this angle is defined as the position of the first phase (a -phase) of the k -set with respect to the α -axis. By applying (5) to (1)-(4), the stator model for IM in (α,β) reference frame becomes:

$$\bar{v}_{sk,\alpha\beta} = R_{sk} \cdot \bar{i}_{sk,\alpha\beta} + \frac{d}{dt} \bar{\lambda}_{sk,\alpha\beta} \quad (6)$$

The rotor equations are transformed into stator stationary reference frame using (5) with $\vartheta_k = \vartheta_r$, where ϑ_r is the rotor electrical position:

$$\bar{0} = R_r \cdot \bar{i}_{r,\alpha\beta} + \frac{d}{dt} \bar{\lambda}_{r,\alpha\beta} - j \cdot \omega_r \cdot \bar{\lambda}_{r,\alpha\beta} \quad (7)$$

where ω_r is the rotor electrical speed.

The IM magnetic model in stationary frame is obtained as:

$$\bar{\lambda}_{sk,\alpha\beta} = L_{l_{sk}} \cdot \bar{i}_{sk,\alpha\beta} + L_m \cdot \sum_{z=1}^n \bar{i}_{sz,\alpha\beta} + L_m \cdot \bar{i}_{r,\alpha\beta} \quad (8)$$

$$\bar{\lambda}_{r,\alpha\beta} = L_{l_r} \cdot \bar{i}_{r,\alpha\beta} + L_m \cdot \sum_{z=1}^n \bar{i}_{sz,\alpha\beta} + L_m \cdot \bar{i}_{r,\alpha\beta} \quad (9)$$

where L_m is the magnetizing inductance.

The IM electromagnetic torque is given by (10) and represents the sum of n outer (vector) products:

$$T = \frac{3}{2} \cdot p \cdot \sum_{z=1}^n (\bar{\lambda}_{sz,\alpha\beta} \times \bar{i}_{sz,\alpha\beta}) \quad (10)$$

According to (6)-(10), the MS approach defines n different stator flux linkage vectors and current vectors and the total electromagnetic torque is the sum of the contributions of the n stator sets that interact with the three-phase rotor. Therefore, the equivalent circuit of the IM corresponding to the MS modeling approach is shown in Fig. 2.

The stator and rotor equations can be referred to a generic rotating reference frame (d,q) at speed ω_e . Indeed, by applying the conventional rotational transformation, the (d,q) voltage equations become:

$$\bar{v}_{sk,dq} = R_{sk} \cdot \bar{i}_{sk,dq} + \frac{d}{dt} \bar{\lambda}_{sk,dq} + j \cdot \omega_e \cdot \bar{\lambda}_{sk,dq} \quad (11)$$

$$\bar{0} = R_r \cdot \bar{i}_{r,dq} + \frac{d}{dt} \bar{\lambda}_{r,dq} + j \cdot (\omega_e - \omega_r) \cdot \bar{\lambda}_{r,dq} \quad (12)$$

The IM magnetic model in rotating (d,q) frame is formally identical with (8-9), with the difference that all vectors (fluxes and currents) are referred to the (d,q) frame instead of the (α,β) stationary reference frame.

III. MODEL PREDICTIVE FORMULATION

The implementation of a predictive system requires first the computation of the machine's state equations and subsequently a good method to discretize them. This procedure is well consolidated for three-phase machines but not for multi three-phase configurations having a higher number of active state variables.

A. Machines's State Equations

The proposed model predictive algorithm uses a DFVC scheme based on the MS-approach [13-16]. Consequently, the stator currents and the stator fluxes must be considered as main state variables. It is necessary to introduce the following preliminary variables:

$$k_r = \frac{L_m}{L_m + L_{l_r}}, \quad k_{sk} = \frac{L_m}{L_m + L_{l_{sk}}}, \quad \tau_r = \frac{L_m + L_{l_r}}{R_r} \quad (13)$$

$$c_k = k_r \cdot L_{l_r} \cdot \sum_{z=1}^n \frac{x_z}{L_{l_{sz}}}, \quad c_z = k_r \cdot L_{l_r} \cdot \frac{x_z}{L_{l_{sz}}} \quad (14)$$

where x_z is a logic value depending by the state of the considered z -set (0 off, 1 on). In this way, it is possible to adapt the equations of the remained active sets after open-windings fault events.

The state equations with the MS approach for a single k three-phase set ($k=1 \dots n$) leads to:

$$L_{eq,k} \cdot \frac{d\bar{i}_{sk,dq}}{dt} = Z_{eq,k} \cdot \bar{i}_{sk,dq} + f_{eq} \cdot \bar{\lambda}_{sk,dq} + k_{v,k} \cdot \bar{v}_{sk,dq} + C_k \quad (15)$$

$$\frac{d}{dt} \bar{\lambda}_{sk,dq} = -R_{sk} \cdot \bar{i}_{sk,dq} + \bar{v}_{sk,dq} - j \cdot \omega_e \cdot \bar{\lambda}_{sk,dq} \quad (16)$$

$$\frac{d}{dt} \bar{\lambda}_{r,dq} = -(\tau_r^{-1} + j \cdot \omega_{slip}) \cdot \bar{\lambda}_{r,dq} + R_r \cdot k_r \cdot \sum_{z=1}^n \bar{i}_{sz,dq} \quad (17)$$

where: $L_{eq,k} = (1 + c_k) \cdot L_{l_{sk}} + k_r \cdot L_{l_r}$

$$Z_{eq,k} = -(R_{eq,k} + j \cdot X_{eq,k})$$

$$R_{eq,k} = R_r \cdot \frac{k_r}{k_{sk}} + R_{sk} \cdot (1 + c_k)$$

$$X_{eq,k} = \omega_r \cdot c_k \cdot L_{l_{sk}} + \omega_{slip} \cdot L_{eq,k}$$

$$f_{eq} = \tau_r^{-1} - j \cdot \omega_r, \quad k_{v,k} = 1 + c_k, \quad \omega_{slip} = \omega_e - \omega_r$$

The term C_k contains the coupling terms between the considered k -set with the other ones $z=1 \dots n, z \neq k$. This is the direct consequence of the application of MS-approach with respect to the conventional Vector Space Decomposition (VSD) [8,13]. The coupling term C_k is computed as:

$$C_k = - \sum_{\substack{z=1 \\ z \neq k}}^n (c_z \cdot \bar{v}_{sz,dq} + Z_{eq,z} \cdot \bar{i}_{sz,dq}) \quad (18)$$

where: $Z_{eq,z} = R_{eq,z} + j \cdot X_{eq,z}$

$$R_{eq,z} = R_r \cdot k_r - R_{sz} \cdot c_z, \quad X_{eq,z} = -\omega_r \cdot c_z \cdot L_{l_{sz}}$$

The equations (15)-(17) represent the complete electromagnetic dynamic model of a multi-three phase machines with a generic number of three-phase sets n . These equations are the starting point for the implementation of any model predictive control.

B. Discretization of the State Equations

The state equations (15)-(17) must be converted into their discrete time equivalents. This operation is not easy to perform, even for a three-phase case. In fact, it is necessary to compute the general relationships of the eigenvalues and related eigenvectors of a high order system. For this reason, in this work the Euler's approximation is proposed.

Independently by the considered equation from the set (15)-(17), each of them has the same structure where from a side there is the derivative of the considered variable \bar{X} while, on the other side, the forcing terms \bar{F} :

$$\frac{d}{dt} \bar{X}(\bar{F}, t) = \bar{F}(t) \quad (19)$$

The Euler's approximation of (19) in order to convert the time domain from continuous to discrete is:

$$\frac{\bar{X}(\tau+1) - \bar{X}(\tau)}{T_s} = \bar{F}(\tau) \Rightarrow \bar{X}(\tau+1) = \bar{X}(\tau) + T_s \cdot \bar{F}(\tau) \quad (20)$$

where T_S is the sample time for the discretization and τ the generic sample time instant. As an example, the application of (20) to (16) leads to:

$$\begin{aligned} \bar{\lambda}_{sk,dq}(\tau+1) &= \bar{\lambda}_{sk,dq}(\tau) + \dots \\ &\dots + T_S \cdot \left[-R_{s,k} \cdot \bar{i}_{sk,dq}(\tau) + \bar{v}_{sk,dq}(\tau) - j \cdot \omega_e(\tau) \cdot \bar{\lambda}_{sk,dq}(\tau) \right] \end{aligned} \quad (21)$$

Since this method is a first-order approximation of the real discrete equations, it is necessary to choose a proper value of sample time T_S . Nevertheless, in an electric drive this value usually corresponds with the switching frequency of the power converter and therefore often predefined. Consequently, the accuracy of the Euler's discretization will depend by the electric fundamental frequency together with a proper estimation of the machine's parameter.

IV. MACHINE CONTROL SCHEME

The application of a model predictive algorithm does not depend on the choice of the control type. In fact, MPC allows at improving the performance of already predefined control scheme by replacing the traditional PI controller with a better selection of the voltage references.

The proposed model predictive algorithm uses a DFVC scheme based on the MS-approach. The DFVC combines the advantages of a direct flux regulation (as for constant frequency direct torque control) with current regulation (as for vector control) [13,15,16]. The main advantage of the MS-approach is the possibility to build a modular machine control where each three-phase set is independently controlled. In this way, post open-winding fault operations or torque sharing operations become easy to perform.

According to the torque demand and the operating speed, the MS-based DFVC aims to controlling n stator flux vectors in n overlapped stator flux frames ($d_{sk}, q_{sk}, k=1,2,\dots,n$), as shown in Fig. 3.

A. Stator Flux and Torque Equations

The machine model in multiple stator flux reference frames ($d_{sk}, q_{sk}, k=1,2,\dots,n$) is described by the equations (15)-(17), where the synchronous speed ω_e corresponds with the pulsation/speed of the considered stator flux vector. In theory, this value must be defined set by set. However, since the machine control aims to set n overlapped stator flux frames, the differences between the three-phase sets can be neglected.

Relevant attention must be given to the stator flux and torque (10),(16) equations. In fact, the DFVC is implemented in rotating stator flux frame and this leads to important simplifications.

In terms of stator flux vectors, each of them is aligned in the own d_{sk} -axis and so all flux q_{sk} -axis components are zero:

$$\frac{d\lambda_{sk}}{dt} = -R_{sk} \cdot i_{sk,ds} + v_{sk,ds} \quad (22)$$

while in terms of total electromagnetic torque:

$$T = \frac{3}{2} \cdot p \cdot \sum_{k=1}^n (\lambda_{sk} \cdot i_{sk,qs}) \quad (23)$$

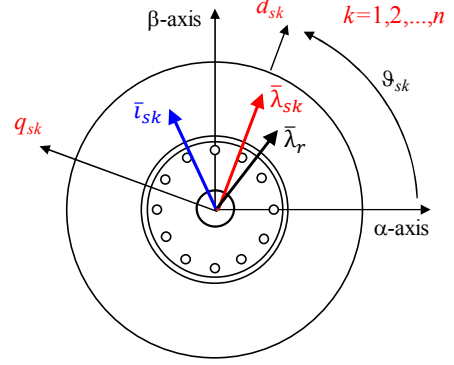


Fig. 3. Multiple direct flux vector control based on MS-approach.

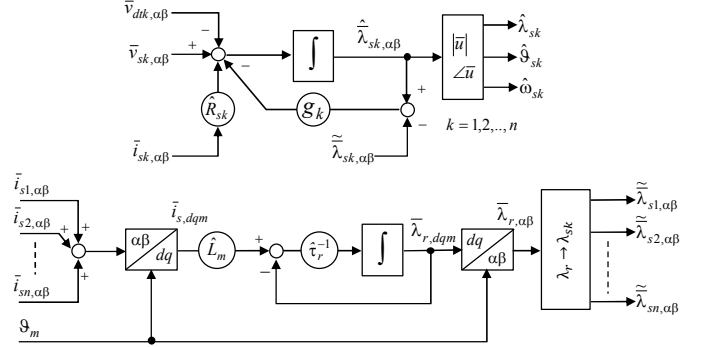


Fig. 4. Stator flux observer.

The model (22),(23) leads to the following considerations:

- The d_{sk} – axis voltage ($v_{sk,ds}$) directly imposes the stator flux magnitude $\lambda_{sk}, k=1,2,\dots,n$.
- The torque contribution of one stator winding set k is controlled by regulating the corresponding q_{sk} – axis current ($i_{sk,qs}$), using the voltage component $v_{sk,qs}, k=1,2,\dots,n$.

B. Stator Flux Observer

The flux observer is shown in Fig. 4. The flux observer estimates n stator flux vectors $\bar{\lambda}_{sk}, k=1,2,\dots,n$, corresponding to the n stator three-phase sets. The flux observer is based on the back-EMF integration at high speed and on the rotor magnetic model at low speed [17].

At low speed, the stator flux vectors are computed from the rotor flux using (7)-(9). The rotor model is sensitive with the rotor time constant τ_r , but this affects only the machine starting. At high speed, the flux estimates depend only on the stator resistances R_{sk} . The detuning on this parameter has very low effects on the flux estimation, so the flux observer is very robust against parameters detuning.

To improve the performance at low speed, a dead-time (DT) compensation scheme has been implemented for each stator set using the solution described in [18].

C. Predictive Direct Flux Vector Control (DFVC) scheme

The proposed predictive DFVC scheme contains n independent modules that are separately implemented in the overlapped stator flux frames ($d_{sk}, q_{sk}, k=1,2,\dots,n$), as shown in Fig. 6.

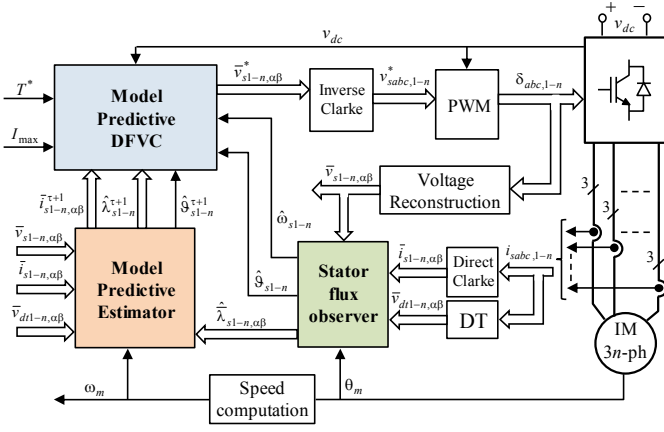


Fig. 5. Predictive direct flux vector control control scheme of a generic multi three-phase machine.

A single DFVC module is operated as for a three-phase machine and does not interact with the other modules.

The reference flux is generated by a Flux-Weakening (FW) block that imposes the rated flux (corresponding to one stator k -set) below the base speed and a flux that depends on the available DC link inverter voltage and the synchronous speed ω_e at flux-weakening. The torque-producing component in stator flux frame is computed for each stator set k as:

$$i_{sk,qs}^* = T^* / \left(\frac{3}{2} \cdot n \cdot p \cdot \hat{\lambda}_{sk} \right), \quad k=1,2,\dots,n \quad (24)$$

The torque producing components for the n stator sets are further limited according to the machine maximum current. The flux computation at flux weakening is implemented as in [15]. The independent flux-current control of the stator sets keeps balanced their currents and allows the operation with one or more stator sets turned off in case of faults.

With respect to a conventional DFVC based on the MS approach [13,16], the application of a predictive algorithm requires additional blocks, as shown in Fig. 5. The first one is the Model Predictive Estimator (MPE) where is performed the prediction of the variable of interest for the next sample time instant $(\tau+1)$. In the MPE block are implemented the state equations (15)-(17) with the application of the Euler's discretization (20). The prediction of the variables is performed in the stationary frame (α,β) in order to use the estimates of the stator flux observer directly. Therefore, the equations (15)-(17) are implemented by setting the synchronous speed ω_e to zero.

The MPE presents a modular structure in order to preserve the control scheme modularity. In fact, it is structured in n predictive estimators where each of them performs the predictive estimation for the dedicated k -set.

From the MPE, the values of stator fluxes and stator currents for the next sample time instant $(\tau+1)$ are obtained. From the predicted values of the stator currents it is possible to estimate the Dead Time (DT) errors of the power converter for the next sample time instant $(\tau+1)$. In this way, it is possible to apply an accurate feed-forward compensation, as shown in Fig. 7. This action leads to relevant improvements in the currents waveforms, especially at low speed and no load-condition.

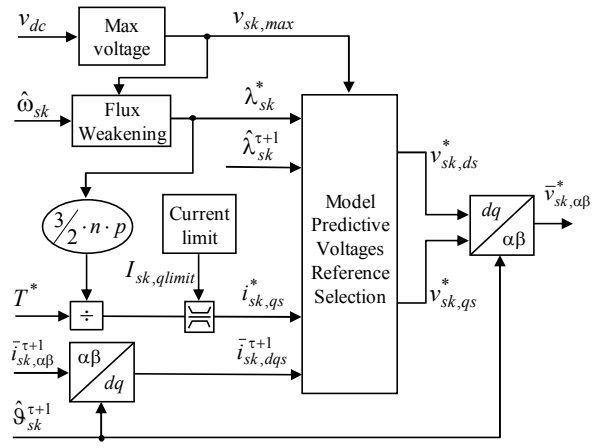


Fig. 6. Predictive DFVC scheme for the k^{th} set.

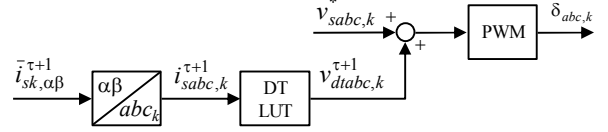


Fig. 7. Predictive Dead Time (DT) errors compensation for the k^{th} set.

For each k -set, the position of the stator flux vector $\hat{\theta}_{sk}^{\tau+1}$, for the next sample time instant $(\tau+1)$, is computed. This is necessary to perform the rotational transformation in order to obtain the (d_{sk},q_{sk}) current values $\bar{i}_{sk,dqs}^{\tau+1}$ for the next sample time instant $(\tau+1)$. The prediction of the angle $\hat{\theta}_{sk}^{\tau+1}$ is also necessary to perform the rotational transformation for the computation of the next sample time $(\tau+1)$ output reference voltages $\bar{v}_{sk,\alpha\beta}^*$.

The predicted value of currents $\bar{i}_{sk,dqs}^{\tau+1}$ and stator flux amplitude $\hat{\lambda}_{sk}^{\tau+1}$, together with the references of stator flux amplitude λ_{sk}^* and q_{sk} -axis current $i_{sk,qs}^*$, are used for the computation of the voltage references $\bar{v}_{sk,\alpha\beta}^*$, as shown in Fig. 6.

D. Predictive Reference Voltages Selection

The proposed model predictive algorithm uses the machine inverse model for the control of the reference variables. Practically, the voltages reference applied at the next sample time instant $(\tau+1)$ establish the evolution of the state variables at the next step $(\tau+2)$:

$$\bar{X}(\tau+2) = \bar{X}(\tau+1) + T_S \cdot \bar{F}(\tau+1) \quad (25)$$

From (25), to set the value of the generic state variable \bar{X} to a target value \bar{X}^* it is necessary to satisfy the (26):

$$\bar{F}^*(\tau+1) = \frac{\bar{X}^* - \bar{X}(\tau+1)}{T_S} \quad (26)$$

Referring to the equations (15)-(17), the application of the (26) corresponds to invert the machine model in order to obtain the voltage references. The proposed method for the computation of the voltages reference is shown in Fig. 8.

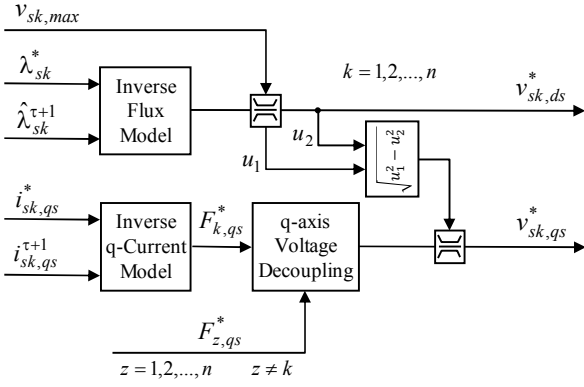


Fig. 8. Voltages reference computation for the k^{th} set.

1) Voltage reference computation on d_{sk} -axis

By considering the (22), the computation of the d_{sk} – axis voltage reference is performed as:

$$v_{sk,ds}^* = R_{sk} \cdot i_{sk,ds}^{\tau+1} + \frac{\lambda_{sk}^* - \hat{\lambda}_{sk}^{\tau+1}}{T_S} \quad (27)$$

The d_{sk} – axis voltage reference, together with the inverter voltage limit define the limits of the q_{sk} – axis component, as the conventional DFVC scheme.

2) Voltage reference computation on q_{sk} -axis

With respect to the d_{sk} – axis component, the computation of the q_{sk} – axis reference voltage must be performed in two steps. In fact, the q_{sk} – axis current equations (15) contains the voltage coupling between the sets. Therefore, first is necessary to compute the linear combinations of voltages reference as function of the q_{sk} – axis current references:

$$k_{v,k} \cdot v_{sk,qs}^* - \sum_{\substack{z=1 \\ z \neq k}}^n c_z \cdot v_{sz,qs}^* = F_{k,qs}^* \quad (28)$$

where:

$$F_{k,qs}^* = \frac{L_{eq,k}}{T_S} \cdot (i_{sk,qs}^* - \hat{i}_{sk,qs}^{\tau+1}) + R_{eq,k} \cdot \hat{i}_{sk,qs}^{\tau+1} + X_{eq,k} \cdot \hat{i}_{sk,ds}^{\tau+1} + \dots \\ \dots + \omega_r \cdot \hat{\lambda}_{sk}^{\tau+1} + \sum_{\substack{z=1 \\ z \neq k}}^n (R_{eq,z} \cdot \hat{i}_{sz,qs}^{\tau+1} + X_{eq,z} \cdot \hat{i}_{sz,ds}^{\tau+1}) + K_{k,comp}^{\tau} \quad (29)$$

In (29) there is a new term called $K_{k,comp}^{\tau}$. It represents the output of an integral regulator. It is computed as:

$$K_{k,comp}^{\tau} = K_{k,comp}^{\tau-1} + T_S \cdot k_{i,k} \cdot (i_{sk,qs}^* - \hat{i}_{sk,qs}^{\tau}) \quad (30)$$

Practically, the (30) represents the integral regulation of the q_{sk} – axis current in a traditional DFVC scheme. Nevertheless, the purpose of this compensation is completely different. In fact, the predictive computation of the variables loses its accuracy at high frequency/speed, caused by the approximation of the Euler's discretization. Furthermore, the predictive algorithm is based on the machine's parameters and consequently is influenced by the estimation errors. These problems cause torque permanent error, especially due by the inaccuracy in the q_{sk} – axis.

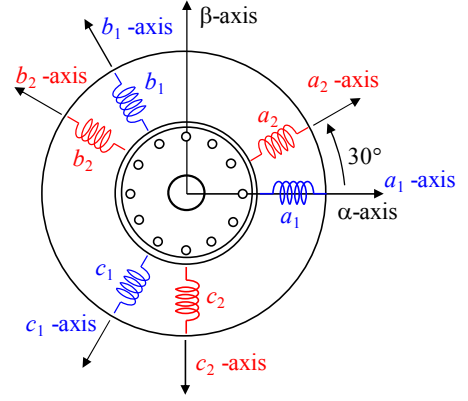


Fig. 9. Asymmetrical 6-phase induction machine configuration (2x3ph).

TABLE I. CHARACTERISTICS OF THE MACHINE

Main Data	
Number of phases	6 (2x3-phase, star connected)
Rated phase voltage	230 Vrms
Generating mode	
Continuous output power	10 kVA
Constant power range	6000 to 15000 rpm
Overload	150% 5 min
Cooling system	forced air ventilation

Through the application of the integral regulation (30), the torque error converges to zero with a dynamic related the value of the integral gain $k_{i,k}$ and the voltage margin of the integral compensator (a good compromise is 5%-10% of the total phase voltage margin). The design of this regulator is not critical. It does not influence the dynamic behavior of the drive but only the steady-state operations.

From the (28) it is necessary to extrapolate the q_{sk} – axis voltage reference $v_{sk,qs}^*$. Therefore, it is necessary to apply the following decoupling operations:

$$\begin{Bmatrix} v_{s1,qs}^* \\ v_{s2,qs}^* \\ \dots \\ v_{sn,qs}^* \end{Bmatrix} = \text{inv} \begin{bmatrix} k_{v,1} & -c_2 & \dots & -c_n \\ -c_1 & k_{v,2} & \dots & -c_n \\ \dots & \dots & \dots & \dots \\ -c_1 & -c_2 & \dots & k_{v,n} \end{bmatrix} \cdot \begin{Bmatrix} F_{1,qs}^* \\ F_{2,qs}^* \\ \dots \\ F_{n,qs}^* \end{Bmatrix} \quad (31)$$

The application of (31) is not critical. In fact, the analytical solutions can be computed offline. In the drive, it is sufficient to implement the analytical results. These are valid also in case of open-winding fault events being the coefficient of matrix defined as (14).

V. EXPERIMENTAL RESULTS

The performance of the proposed control has been validated with an asymmetrical six-phase induction machine using a double-three-phase stator winding configuration. The main features of the machine are shown in Table I [16]. The stator has 6 phases with two slot/pole/phase, forming a double-three-phase winding with relative shift of 30 electrical degrees among the two three-phase sets ($a_k b_k c_k$), $k=1,2$, as shown in Fig. 9.



Fig. 10. Machine under test (right) and the driving machine (left)

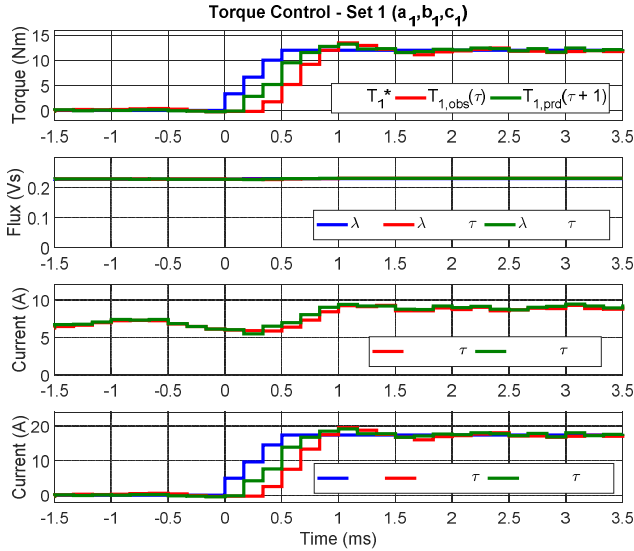


Fig. 11. Fast torque transient from no-load up to 150% rated torque (24Nm) at -6000 rpm, Set 1. From top to bottom: reference torque, observed torque and predicted torque (Nm); reference stator flux, observed stator flux and predicted stator flux; observed d_{s1} -axis current and predicted d_{s1} -axis current; reference q_{s1} -axis current, observed q_{s1} -axis current and predicted q_{s1} -axis current.

The machine has been mounted on a test rig for development purposes. The shaft of the machine prototype is connected with a driving machine (Fig. 10). The power converter consists of two independent three-phase inverter IGBT power modules fed by a single DC power source of 550V. All inverter units are based on the Infineon 100A/1200V, MIPAQ three-phase IGBT power module. The digital controller is the dSpace DS1103 development board that uses a dedicated FPGA-based interface to communicate with the inverter modules through optical fibers. The sampling frequency and the inverters switching frequency have been set at 6 kHz.

A. Healthy operation

The machine has been tested in generation mode with a negative speed of -6000 rpm imposed by the prime mover (speed controlled), while the machine is torque controlled. The generator operation in healthy conditions is shown in Figs. 11-13 for fast torque transient (40Nm/ms) from zero up to 24 Nm (0 to 15kW mech., 150% of the rated value). It can be noted how the two three-phase sets are perfectly balanced with a fair distribution of the total power (12Nm - 7.5kW mech. for each set), as can be seen in Fig. 13. It can be noted the right prediction of torque, currents and stator fluxes, as shown in Figs. 11-12. Furthermore, the perfect torque response (as the well-known DBTFC).

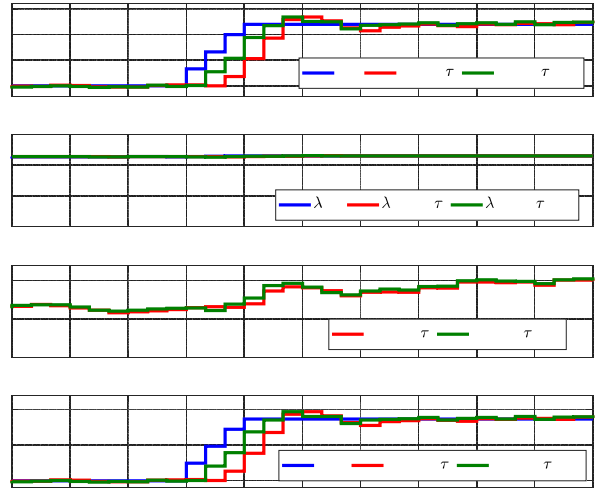


Fig. 12. Fast torque transient from no-load up to 150% rated torque (24Nm) at -6000 rpm, Set 2. From top to bottom: reference torque, observed torque and predicted torque (Nm); reference stator flux, observed stator flux and predicted stator flux; observed d_{s2} -axis current and predicted d_{s2} -axis current; reference q_{s2} -axis current, observed q_{s2} -axis current and predicted q_{s2} -axis current.

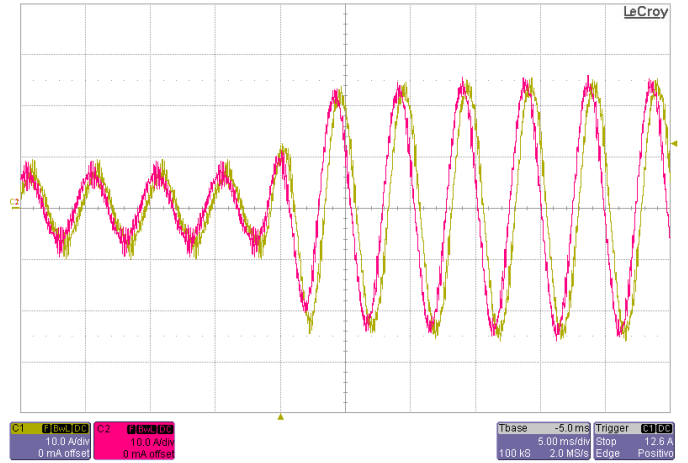


Fig. 13. Fast torque transient from no-load up to 150% rated torque (24Nm) at -6000 rpm. Ch1: i_{a1} (10A/div), Ch2: i_{a2} (10A/div).

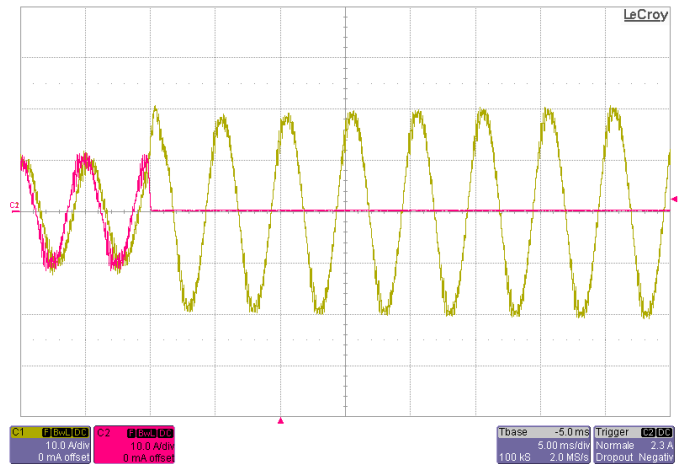


Fig. 14. Inverter 2 shut off during generation mode at -6000rpm and 10Nm. Ch1: i_{a1} (10A/div), Ch2: i_{a2} (10A/div).

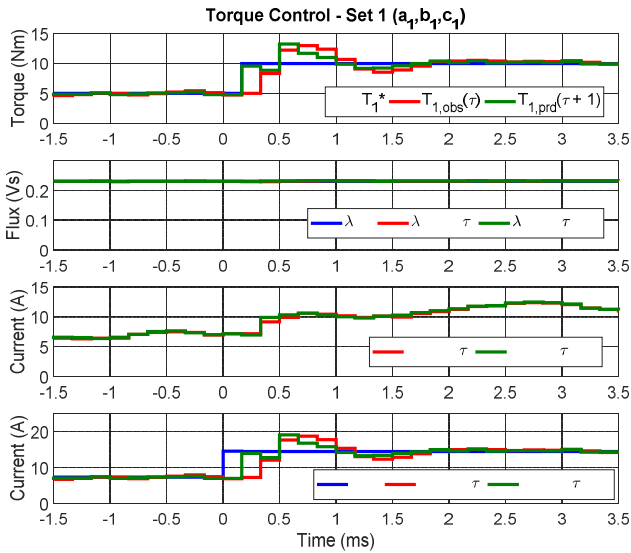


Fig. 15. Inverter 2 shut off during generation mode at -6000rpm and 10Nm. Set 1. From top to bottom: reference torque, observed torque and predicted torque (Nm); reference stator flux, observed stator flux and predicted stator flux; observed d_{s1} -axis current and predicted d_{s1} -axis current; reference q_{s1} -axis current, observed q_{s1} -axis current and predicted q_{s1} -axis current.

B. Faulty operation

The drive “fault ride-through” capability when one inverter unit is suddenly disabled is shown in Figs. 14-16 (inverter 2 off), with fast and good dynamic. The healthy unit exhibits sinusoidal currents that increase in order to keep the same torque and machine flux, as shown in Fig. 14. This is the proof of the modularity of the MS-based control schemes, with the maximum degree of freedom in the control of the single three-phase sets.

VI. CONCLUSIONS

The paper proposes a model predictive control (MPC) for multiphase induction machine configured as multiple three-phase structures. The predictive algorithm is implemented on the basic structure of the Direct Flux Vector Control (DFVC) scheme for simultaneous flux and torque control. The performance of the proposed control has been validated with a double-three-phase induction machine. The experimental results demonstrate the feasibility of the proposed drive solution both in healthy and faulty operations (open-winding fault events).

REFERENCES

- [1] P. Correa, M. Pacas, J. Rodriguez, “Predictive Torque Control for Inverter-Fed Induction Machines”, *IEEE Trans. Ind. Electron.*, vol. 54, no. 2, 2007, pp. 1073-1079.
- [2] M. Preindl, S. Bolognani, “Model Predictive Direct Torque Control with Finite Control Set of PMSM Drive Systems, Part 1&2”, *IEEE Trans. Ind. Informatics*, vol. 9, no. 4 & no. 2, 2013, pp. 1912-1921 & pp. 648-657.
- [3] B. Boazzo, G. Pellegrino, “Predictive Direct Flux Vector Control of Permanent Magnet Synchronous Motor Drives”, *IEEE-ECCE*, 2013, pp. 2086-2093.
- [4] Y. Zhang, H. Yang, “Model Predictive Torque Control of Induction Motor Drives With Optimal Duty Cycle Control”, *IEEE Trans. Power Electron.*, vol. 29, no. 12, 2014, pp. 6593-6603.
- [5] C. A. Rojas, J. Rodriguez, F. Villarroel, J. R. Espinoza, C. A. Silva, M. Trincado, “Predictive Torque and Flux Control Without Weighting Factors”, *IEEE Trans. Ind. Elect.*, 2013, vol. 60, no. 2, pp. 681-590.

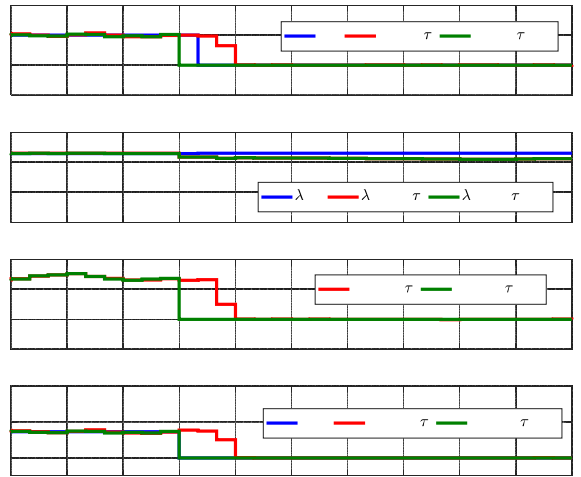


Fig. 16. Inverter 2 shut off during generation mode at -6000rpm and 10Nm. Set 2. From top to bottom: reference torque, observed torque and predicted torque (Nm); reference stator flux, observed stator flux and predicted stator flux; observed d_{s2} -axis current and predicted d_{s2} -axis current; reference q_{s2} -axis current, observed q_{s2} -axis current and predicted q_{s2} -axis current.

- [6] S. A. Odhano, A. Formentini, P. Zanchetta, R. Bojoi, A. Tenconi, “Finite Control Set and Modulated Predictive Flux and Current Control for Induction Motor Drives”, *Conf. Rec. IEEE-IECON*, 2016, pp. 2796-2801.
- [7] J. W. Kelly, E. G. Strangas, and J. M. Miller, “Multi-phase inverter analysis”, *Conf. Rec. IEEE-IEMDC*, 2001, pp. 147-155.
- [8] Y. Zhao and T.A. Lipo, “Space vector PWM control of dual three-phase induction machine using vector space decomposition”, *IEEE Trans. Ind. Appl.*, 1995, vol. 31, no. 5, pp. 1100-1108.
- [9] F. Barrero, J. Prieto, E. Levi, R. Gregor, S. Toral, M.J. Duran, and M. Jones, “An Enhanced Predictive Current Control Method for Asymmetrical Six-Phase Motor Drives”, *IEEE Trans. Ind. Electron.*, 2011, vol. 58, no. 8, pp. 3242-3252.
- [10] Y. Wang, S. Tobayashi, and R.D. Lorenz, “A Low-Switching-Frequency Flux Observer and Torque Model of Deadbeat-Direct Torque and Flux Control on Induction Machine Drives”, *IEEE Trans. Ind. Applicat.*, vol. 51, no. 3, 2015, pp. 2255-2267.
- [11] W. Cao, B. Mecrow, G. Atkinson, J. Bennett, and D. Atkinson, “Overview of Electric Motor Technologies Used for More Electric Aircraft (MEA)”, *IEEE Trans. Ind. Electron.*, 2011, vol. 59, no. 9, pp. 3523-3531.
- [12] R.H. Nelson and P.C. Krause, “Induction machine analysis for arbitrary displacement between multiple winding sets”, *IEEE Trans. Power Appl. and Systems*, vol. PAS-93, 1974, pp. 841-848.
- [13] S. Rubino, R. Bojoi, A. Cavagnino, and S. Vaschetto, “Asymmetrical Twelve-Phase Induction Starter/Generator for More Electric Engine in Aircraft”, *Conf. Rec. IEEE-ECCE*, 2016, pp. 1-8.
- [14] R. Bojoi, S. Rubino, A. Tenconi, S. Vaschetto, “Multiphase electrical machines and drives: A viable solution for energy generation and transportation electrification”, *EPE 2016*, pp. 632 – 639.
- [15] G. Pellegrino, R. Bojoi, and P. Guglielmi, “Unified Direct-Flux Vector Control for AC Motor Drives”, *IEEE Trans. Ind. Appl.*, 2011, vol. 47, no. 5, pp. 2093-2102.
- [16] R. Bojoi, A. Cavagnino, A. Tenconi and S. Vaschetto, “Control of Shaft-Line-Embedded Multiphase Starter/Generator for Aero-Engine”, *IEEE Trans. Ind. Electron.*, vol. 63, no.1, 2016, pp.641-652.
- [17] P.L. Jansen and R.D. Lorenz, “A Physically Insightful Approach to the Design and Accuracy Assessment of Flux Observers for Field Oriented Induction Machine Drives”, *IEEE Trans. Ind. Appl.*, vol. 30, no.1, pp. 101-110, 1994.
- [18] R. Bojoi, E. Armando, G. Pellegrino, and S.G. Rosu, “Self-commissioning of inverter nonlinear effects in AC drives”, *Conf. Rec. IEEE ENERGYCON*, 2012, pp. 213-218.